

Lawrence Berkeley National Laboratory

Recent Work

Title

Precision Alignment of the Advanced Light Source U5.0 and U8.0 Undulators

Permalink

<https://escholarship.org/uc/item/0vw8s5kf>

Authors

Humphries, D.

Chin, J.

Connors, R.

et al.

Publication Date

1993-07-01



Lawrence Berkeley Laboratory

UNIVERSITY OF CALIFORNIA

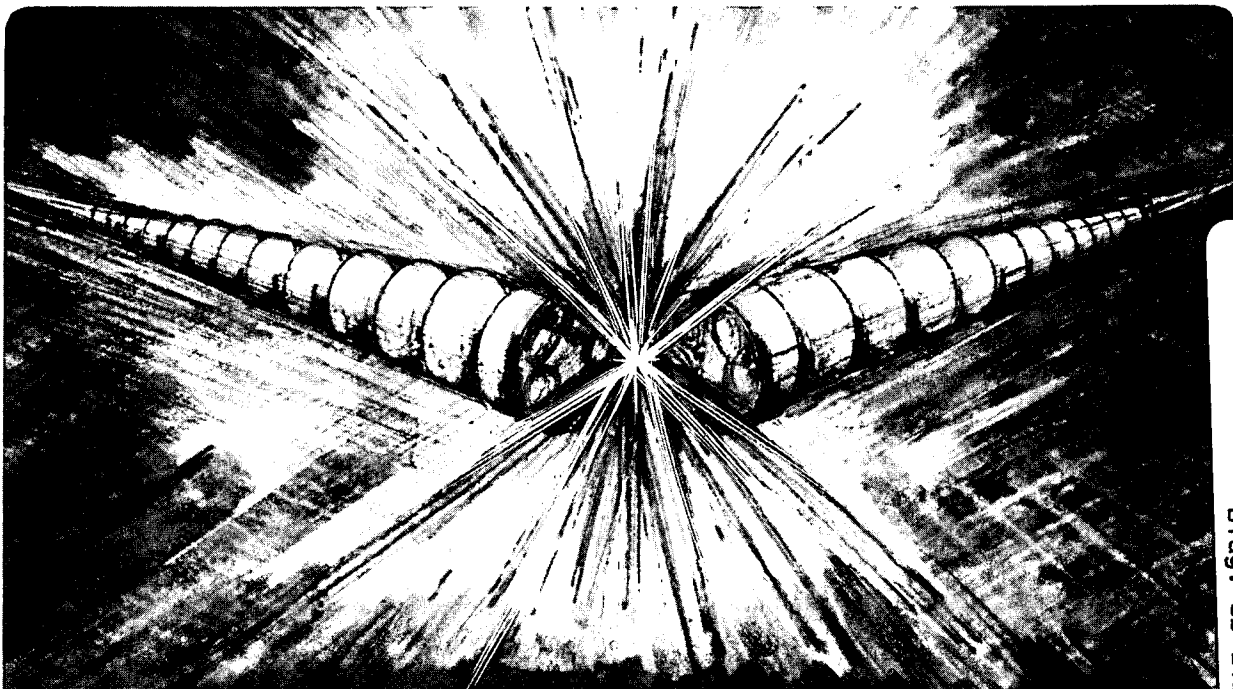
Accelerator & Fusion Research Division

Presented at the SPIE 1993 International Symposium on
Optical Applied Science and Engineering, San Diego, CA,
July 11-16, 1993, and to be published in the Proceedings

Precision Alignment of the Advanced Light Source U5.0 and U8.0 Undulators

D. Humphries, J. Chin, R. Connors, J. Cummings, T. Keffler,
W. Gath, E. Hoyer, B. Kincaid, and P. Pipersky

July 1993



REFERENCE COPY
Does Not Circulate
Bldg. 50 Library.
COPY 1

LBL-33237

DISCLAIMER

This document was prepared as an account of work sponsored by the United States Government. While this document is believed to contain correct information, neither the United States Government nor any agency thereof, nor the Regents of the University of California, nor any of their employees, makes any warranty, express or implied, or assumes any legal responsibility for the accuracy, completeness, or usefulness of any information, apparatus, product, or process disclosed, or represents that its use would not infringe privately owned rights. Reference herein to any specific commercial product, process, or service by its trade name, trademark, manufacturer, or otherwise, does not necessarily constitute or imply its endorsement, recommendation, or favoring by the United States Government or any agency thereof, or the Regents of the University of California. The views and opinions of authors expressed herein do not necessarily state or reflect those of the United States Government or any agency thereof or the Regents of the University of California.

PRECISION ALIGNMENT OF THE ADVANCED LIGHT SOURCE U5.0 AND U8.0 UNDULATORS*

D. Humphries, J. Chin, R. Connors, J. Cummings, T. Keffler, W. Gath, E. Hoyer, B. Kincaid, and P. Pipersky

Advanced Light Source
Accelerator and Fusion Research Division
Lawrence Berkeley Laboratory
University of California
Berkeley, CA 94720

July 1993

Paper Presented at the SPIE 1993 International Symposium on Optical Applied Science and Engineering
San Diego, CA
July 11-16, 1993

*This work was supported by the Director, Office of Energy Research, Office of Basic Energy Sciences, Materials Sciences Division of the U.S. Department of Energy, under Contract No. DE-AC03-76SF00098.

Precision alignment of the Advanced Light Source U5.0 and U8.0 undulators

D. Humphries, J. Chin, R. Connors, J. Cummings, T. Keffler, W. Gath, E. Hoyer, B.M. Kincaid, P. Pipersky

Lawrence Berkeley Laboratory, University of California
One Cyclotron Road, Berkeley, California 94720

ABSTRACT

The U5.0 and U8.0 undulators for the Advanced Light Source (ALS) incorporate 4.6-m-long, hybrid-configuration magnetic structures. The structures consist of modules with half-period pole assemblies mounted on 0.8-m-long aluminum mounts, which are in turn attached to continuous steel backing beams. The vertical and longitudinal alignment tolerances for the poles of these structures are 25 microns and 50 microns, respectively, over the entire 4.6-m length of the devices. To meet these tolerances, the modules were first aligned individually using an automated coordinate measurement machine and shimming techniques. Several adjustment iterations were required for each module. Averaging and three-dimensional linear least-squares fitting techniques were employed to establish statistically based error reference planes. Graphical spread sheets were used to create representations of vertical and longitudinal pole position errors for alignment.

The adjusted modules were installed on the backing beams and aligned relative to each other using laser interferometer techniques. The longitudinal positions of all poles of each module were measured using a simple linear interferometer and associated optics. Because of the differential expansion coefficient between the aluminum modules and steel backing beam, a bilinear temperature-compensation function was applied to the position data to predict periodicity errors at a predetermined operating temperature, which is generally higher than temperatures in assembly and measurement areas.

Vertical alignment of the periodic modules was performed by generating vertical pole position error profiles of the full 4.6-m structures. These profiles were obtained by using an angular interferometer and performing an integrated angle calculation on the data. Least-squares-fit planes for each module were calculated and used in making differential vertical and angular adjustments. Repeatability error for these measurements was typically less than 3 microns. In addition, by using difference techniques, systematic profile variations of 1 micron have been resolved.

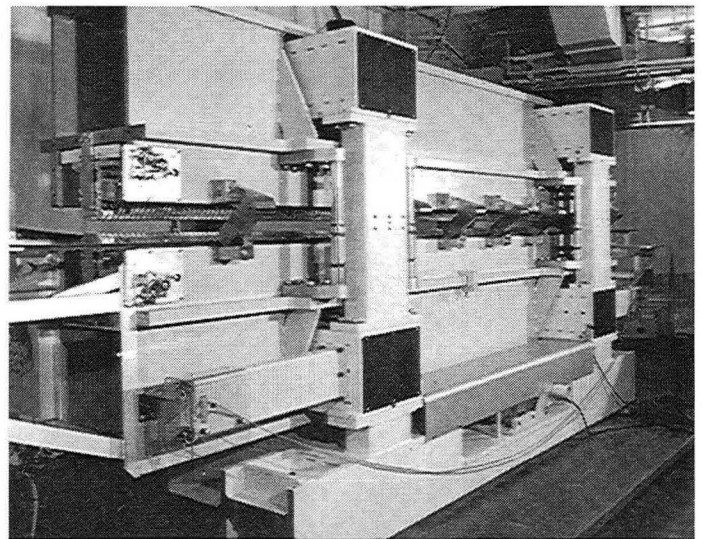
This paper presents techniques, calculations, and alignment results.

1. MECHANICAL CONFIGURATION

The U5.0 and U8.0 undulators for the ALS¹ incorporate 4.6-m-long, hybrid-configuration magnetic structures. The structures consist of modules with half-period pole assemblies (hereafter called "pole assemblies") mounted on thick aluminum plates, which are in turn attached to continuous steel backing beams. The two backing beams with their attached magnetic structures are mounted in a support structure as shown in Figure 1, the IDA U5.0 insertion device near completion.

1.1. Pole assemblies

Each pole assembly consists of a vanadium permendur pole and six Nd-Fe-B permanent magnet blocks surrounded by an aluminum keeper. The poles are attached to the aluminum keeper with non-magnetic stainless-steel dowel pins after machining and heat treating. The permanent magnet blocks are carefully positioned relative to the pole face, then bonded into these assemblies to produce the basic half-period magnetic units of the undulators.²



CBB 910-862D

Figure 1. IDA U5.0 insertion device.

An isometric representation of a pole assembly is shown in Figure 2. The orthographic representation of the assembly in Figure 3 illustrates the independent right and left adjustment spacers for longitudinal positioning and the single locating dowel pin centered at the bottom of the aluminum keeper.

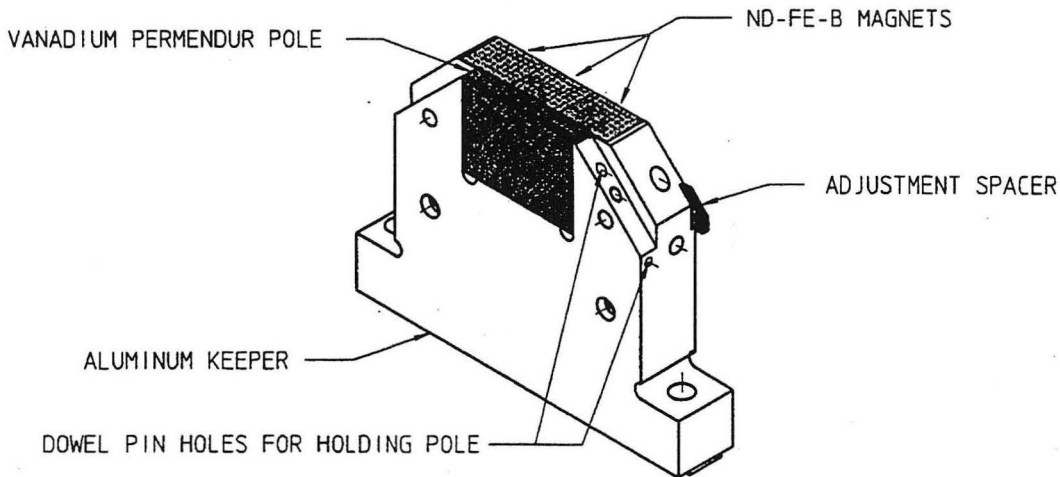


Figure 2. Isometric of half period pole assembly.

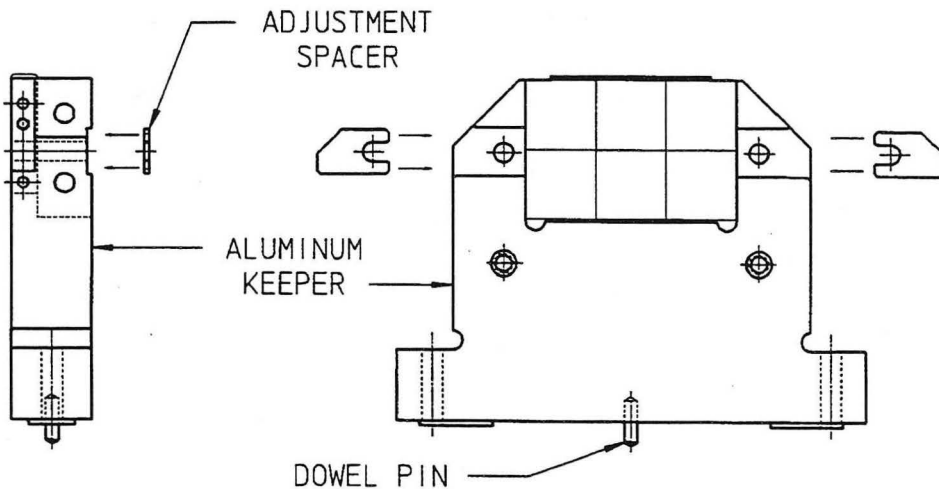
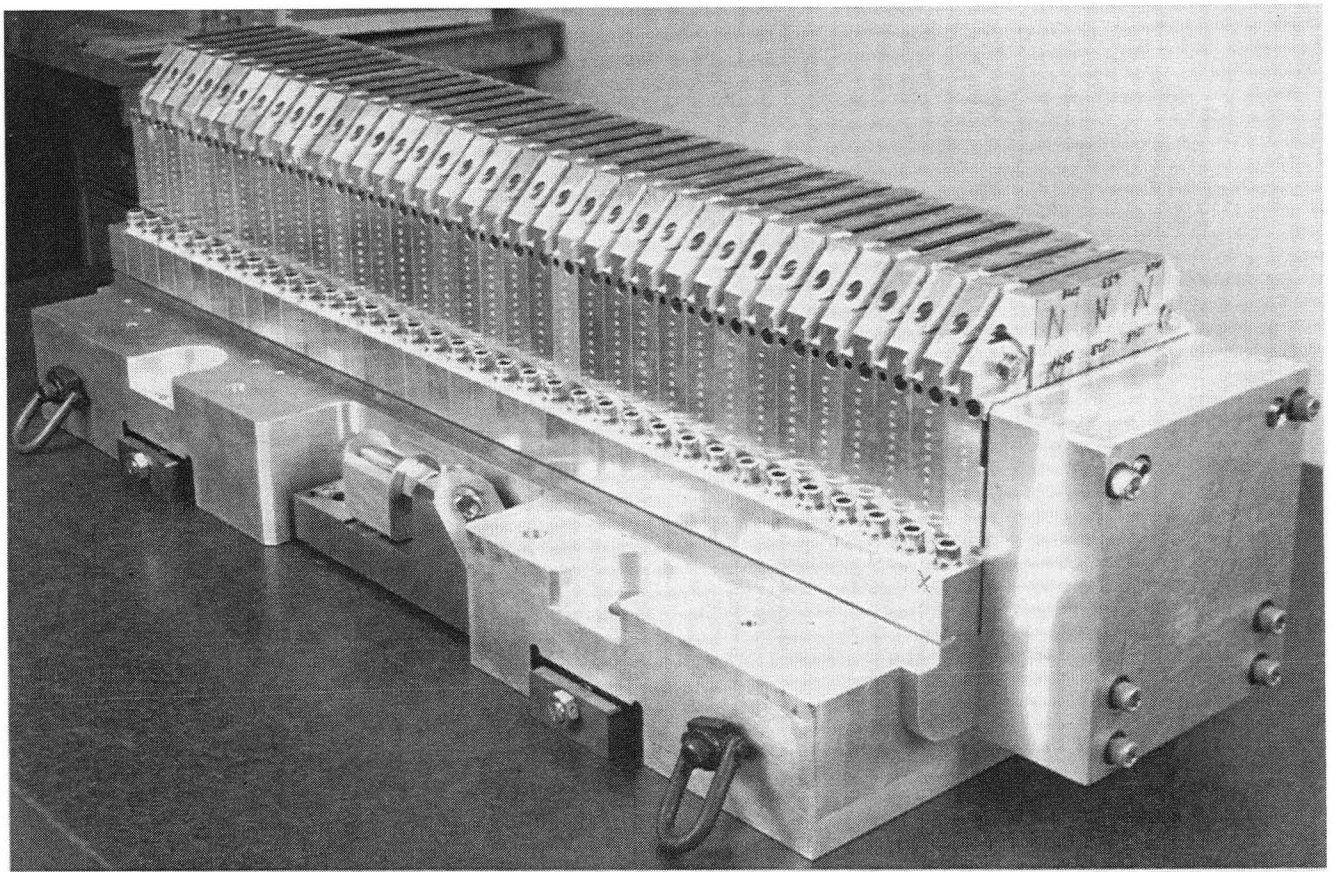


Figure 3. Orthographic view of half-period pole assembly.

1.2. Periodic modules

Completed pole assemblies are selected and attached to aluminum plates or "pole mounts" to form magnetic-structure modules or "periodic modules." A typical periodic module is shown in Figure 4 and details are given in Figure 5. There are five of these modules on each of the two backing beams of the device. Also shown in Figure 5 is the coordinate system, which is the convention used for the alignment and for the magnetic structure in general.



CBB 9110-8213

Figure 4. Periodic module of the magnetic structure with alignment brace attached.

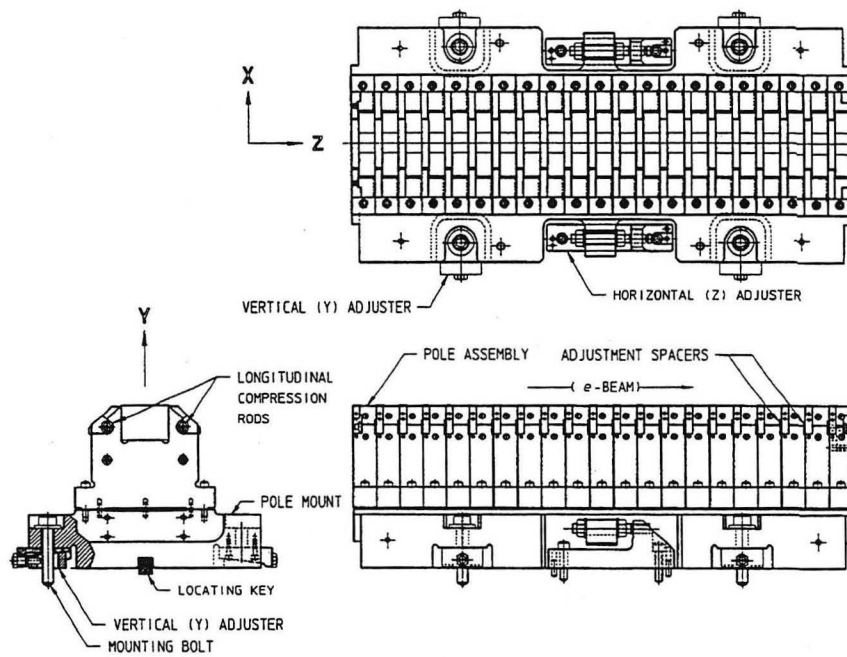


Figure 5. Orthographic view of periodic module of the magnetic structure.

The longitudinal (Z) and vertical (Y) adjuster mechanisms can be seen in Figure 5. These are shown in greater detail in Figures 6a and 6b.

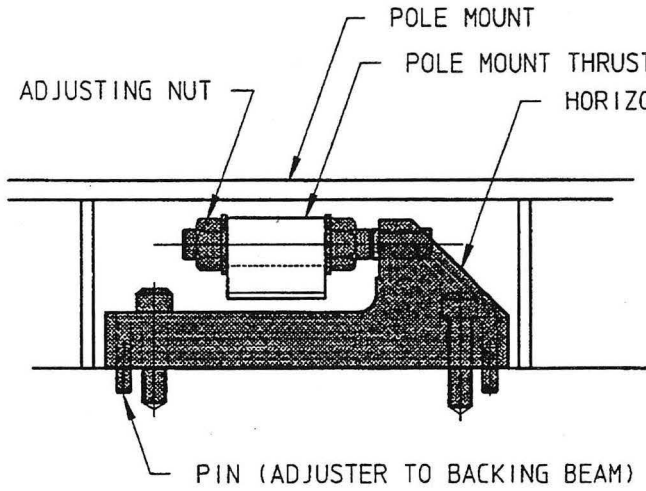


Figure 6a. Longitudinal (Z) adjuster.

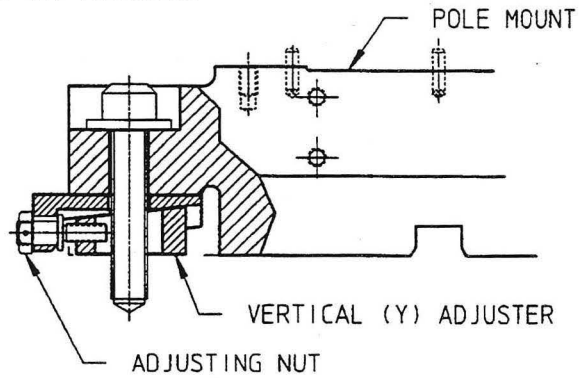


Figure 6b. Vertical (Y) adjuster.

1.3. End modules

In addition to the periodic modules there are two "end modules" that complete the magnetic structure. These consist of a limited number of standard and special pole assemblies which are mounted on their own special pole mounts as shown in Figures 7a and 7b. A portion of the backing beam and the end module vertical adjuster interface can also be seen in these Figures.

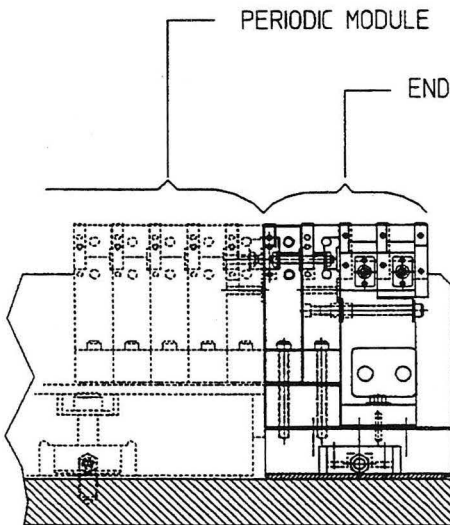


Figure 7a. Side view of magnetic-structure end module.

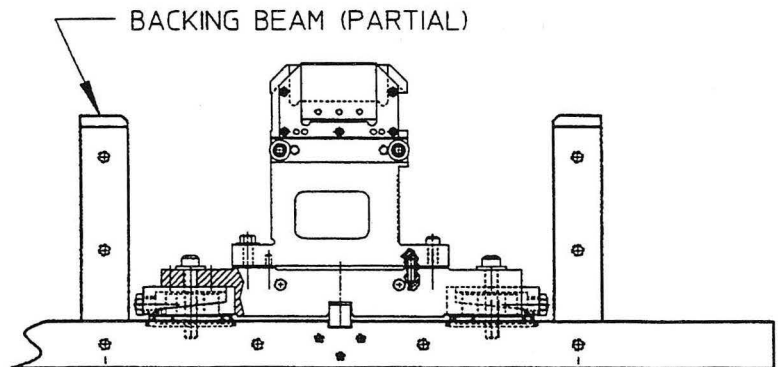
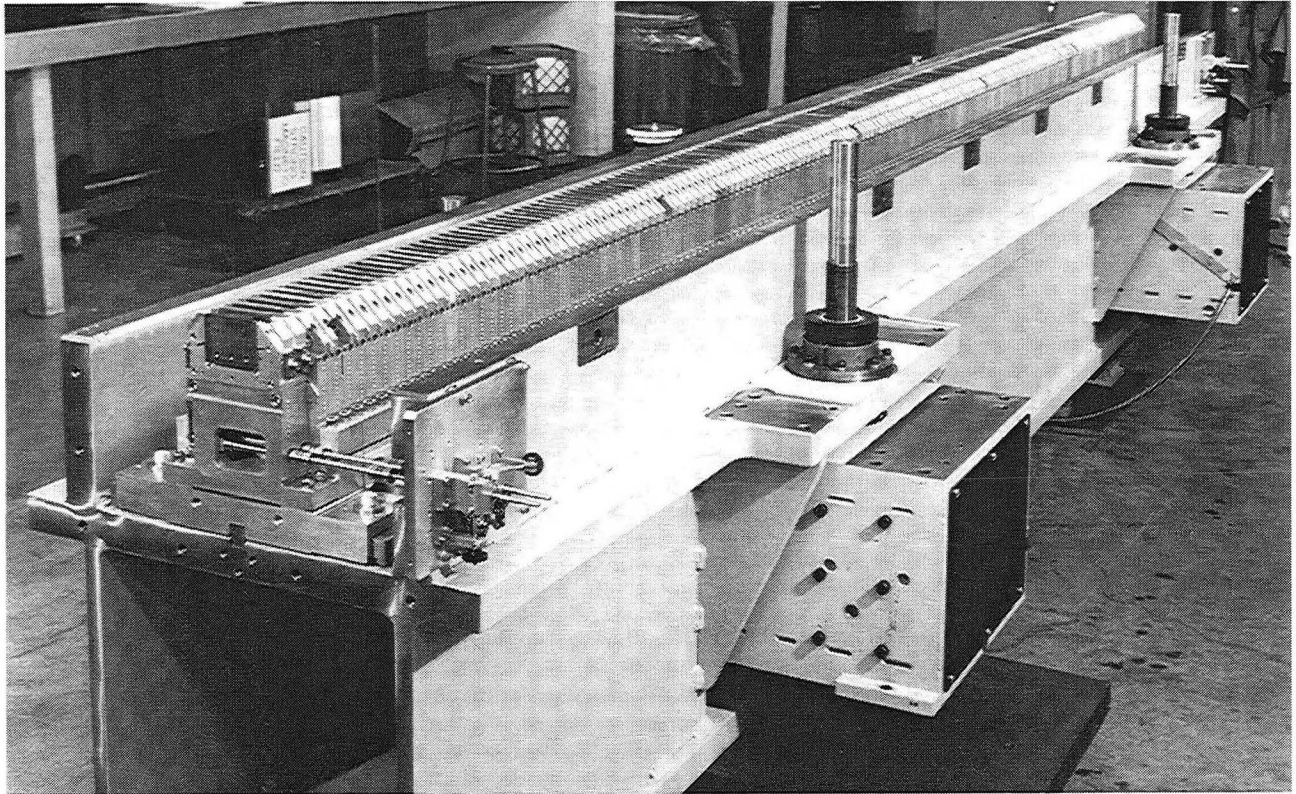


Figure 7b. End view and interface to backing beam.

1.4. Magnetic structure/backing beam assembly

The end and periodic modules are mounted to a large, rigid, backing beam as shown in the photograph in Figure 8. Figures 9a and 9b give side and cross-sectional views of these 4.6-m-long combined structures.



CBB 922-1132

Figure 8. Photograph of magnetic structure installed in backing beam.

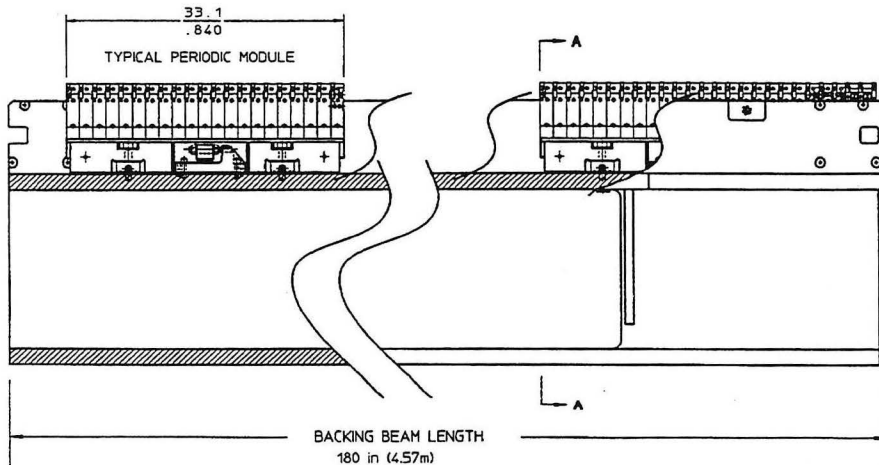


Figure 9a. Side view of magnetic structure installed in backing beam.

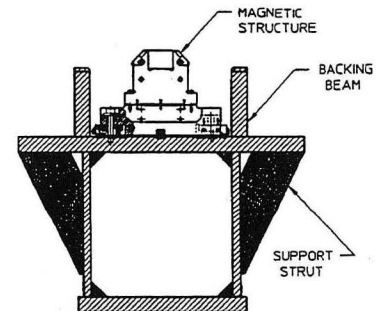


Figure 9b. Cross section.

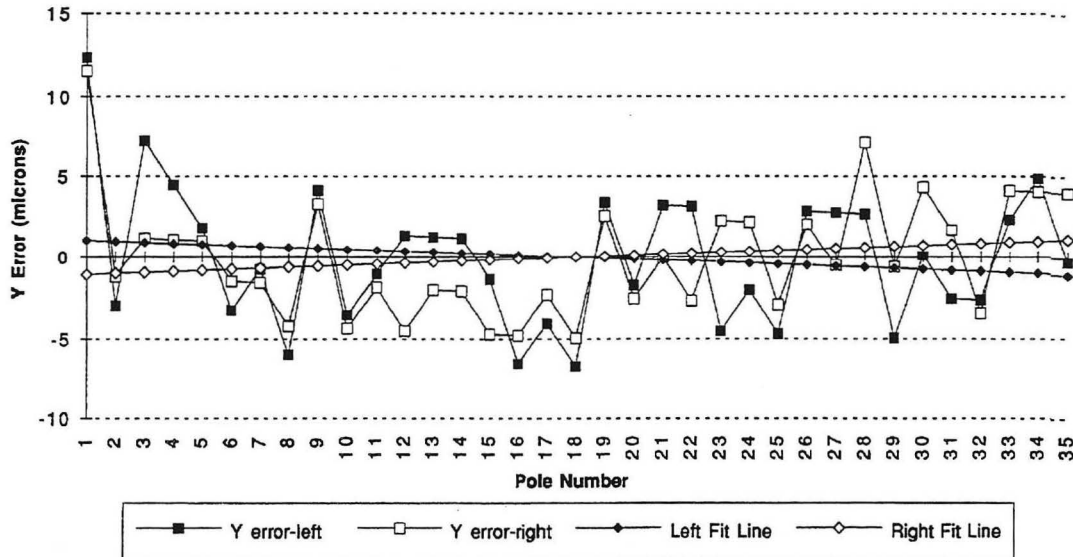


Figure 11. Vertical (Y) pole position error graph.

4. ALIGNMENT OF MAGNETIC STRUCTURE ON BACKING BEAMS

4.1. Installation and adjustment mechanisms

After the internal alignment of the modules is complete, five periodic modules and two end modules are installed on each of the two backing beams. Figures 7 through 9 show various views of this assembly. The end views in Figures 5 and 7 show a locating key at the bottom center of the pole mount which provides lateral or X direction restraint of the magnetic structure in the backing beam. The magnetic structure has the largest position tolerance budget (~500 microns) in the X direction. This tolerance is large enough to be met by location specification of the keyways in the backing beam and in the bottom of the pole mounts, and adjustment of the backing beams in the support and drive system.⁶

The longitudinal position of the periodic modules is adjusted and maintained after adjustment by means of two longitudinal (Z) adjusters located on either side of the module. These mechanisms are shown in Figures 4, 5, and 6a. These adjusters consist of precision nuts and washers on a fine threaded shaft and have an incremental positioning capability of approximately 3 microns. The end modules are located longitudinally by external pusher mechanisms that are removed after final adjustments have been made.

Vertical position, pitch, and roll of the modules are controlled by four vertical (Y) adjusters. These are shown in Figures 4, 5, 6b, and 7. Periodic modules use four of these adjusters while the end modules use either two for the U5.0 insertion device or three for the U8.0 insertion device. All vertical adjuster mechanisms are coincident with the mounting bolts that attach the modules to the backing beams.

4.2. Initial alignment of modules

The magnetic-structure modules are initially aligned on the backing beam using a conventional (non-laser) optical level to achieve vertical pole positioning.⁷ A ceramic monument is placed on appropriate pole faces and sighted through the level to determine pole heights relative to the global reference plane of the level. The modules are adjusted so that their least-squares-fit reference planes (described in section 3.3) lie close to the same plane parallel to the global reference plane. The accuracy of the optical level allows fit plane alignment to within approximately 200 microns.

The transverse roll alignment of the modules is incidentally completed during this initial alignment process. The geometry of the pole face array, i.e., narrow pole face width relative to length of module, results in angular roll alignment of approximately 0.2 mrad by this method. No further roll adjustments are made after this stage in the alignment process.

The initial longitudinal (Z) alignment of the magnetic structure modules is accomplished by means of simple gauge blocks or plastic gauge sheets inserted between adjacent modules. This method allows longitudinal alignment to within approximately 200 microns, which is adequate for this stage of alignment.

4.3. Final vertical alignment of modules

The goal of the final vertical alignment process is to align the least-squares-fit planes of the periodic modules to within 5 microns. It is an iterative process that uses a laser interferometer measurement system⁸ to generate high-accuracy error profiles of the vertical pole face positions. For this measurement an angular retroreflector was moved from pole to pole and relative angles were recorded to a file. The angle data were then transferred to a graphical spreadsheet for analysis. An integrated-angle, pole-height profile of the entire magnetic structure (seven modules) was calculated. In addition, least-squares-fit planes were calculated for each of the five periodic modules and for the two end modules. An example of a complete error profile with calculated module fit planes is shown in Figure 12.

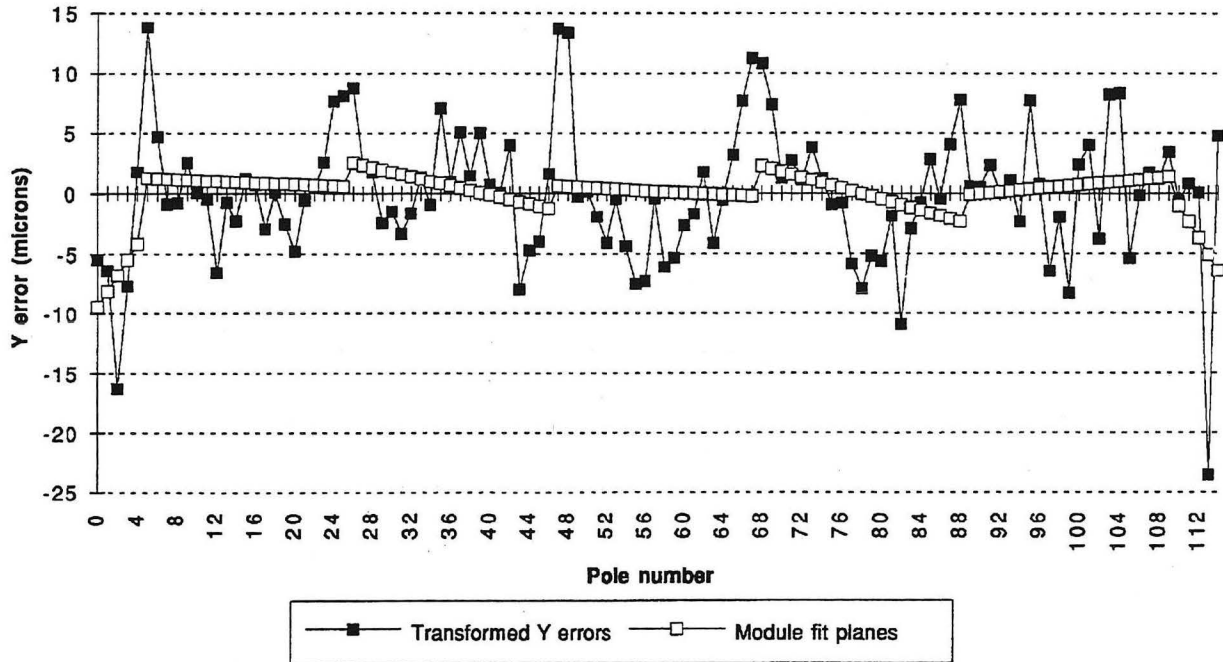
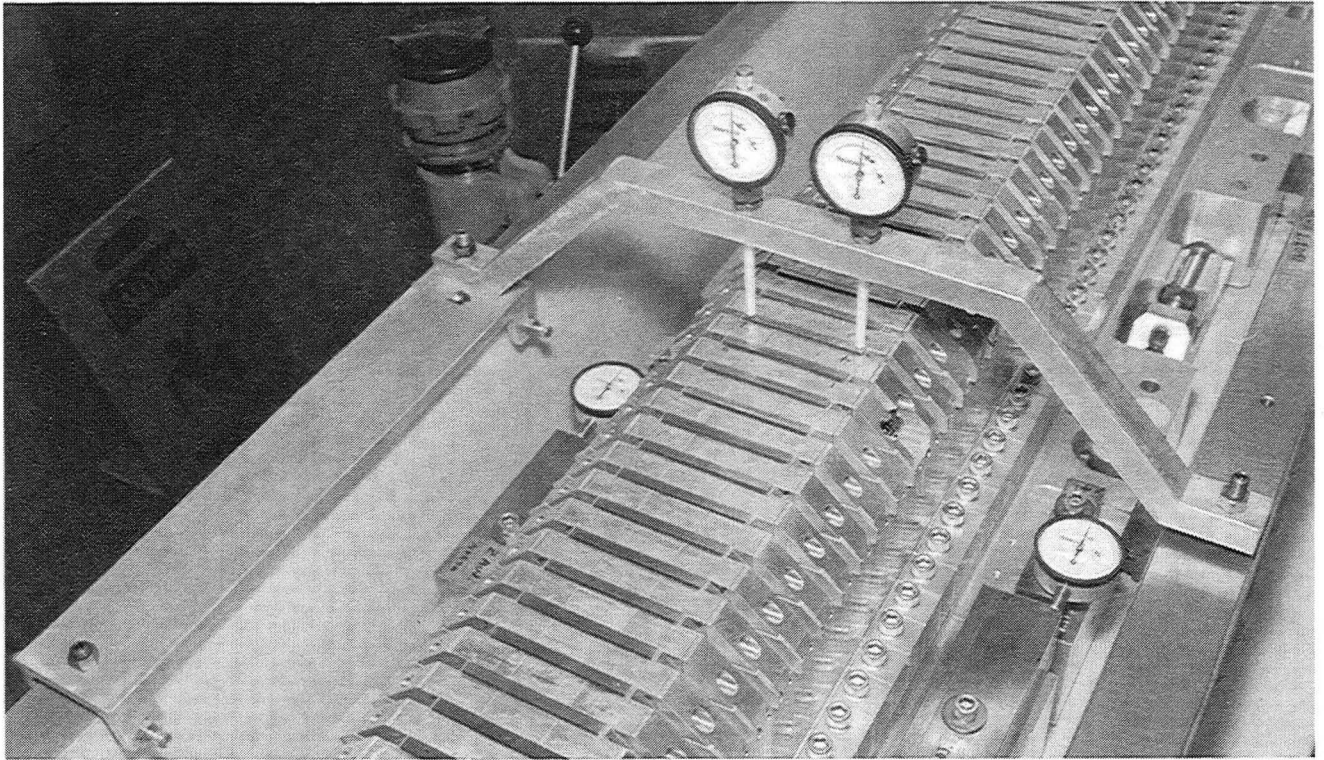


Figure 12. Laser-interferometer vertical (Y) error profile with least-squares error plane for each module.

The object of this phase of the alignment is to align the fit planes of the modules. The graphical representation of the fit planes is used directly to determine differential movements of the individual modules that will bring the calculated-fit planes into alignment. Once the desired differential movements are known, an array of precision (2-micron) dial indicators is placed in contact with appropriate pole faces of a module. The indicator array is shown in Figure 13. Each indicator is preset to read the desired differential movement for that location of that pole face. The module is then carefully repositioned by means of the vertical adjuster mechanisms until the dial indicators read zero.

This process is repeated for each module on the backing beam. After all the modules have been adjusted, the magnetic structure is measured again with the laser interferometer system and a new profile and fit plane set is generated. If the fit plane alignment error is still unacceptably large, the modules are again differentially moved. This process is repeated until the fit planes are sufficiently aligned or until all individual pole position vertical errors are within the specified tolerance. This process typically results in alignment of the fit planes to within 5 microns after two iterations. The residual vertical pole position errors that resulted from the internal CMM alignment of the individual modules are typically larger by a factor of five than the final fit plane misalignment error resulting from the laser interferometry process.

In order to test for and ensure the accuracy of the laser profiles, two complete scans are made for the generation of each profile. The typical *maximum* repeatability error incurred is 4 microns over the entire 4.6-meter length of the scan. The standard deviation of the repeatability error is typically closer to 1.5 microns.



XBC 924-2578

Figure 13. Dial indicator array for differential movements of modules.



CBB 924-2881

Figure 14. Longitudinal pole position measurements with laser-interferometer system.

4.4. Final longitudinal alignment of modules

The longitudinal pole positions are determined by a somewhat simpler laser interferometer system involving a single movable retroreflector and interferometer/reference reflector combination. These measurements are complicated, however, by a differential temperature expansion effect: the magnetic-structure modules are partly aluminum and expand and contract as aluminum — more than the steel backing beam for a given change in temperature.

This effect is compounded in the case of the ALS by the fact that the specified (and controlled) operating temperature of the storage ring tunnel is 24 degrees C while a typical ambient temperature for assembly areas is about 20 degrees C with significant daily and seasonal fluctuations.

Because of these complications, a bilinear temperature-compensation function was developed to allow longitudinal adjustment of the modules at arbitrary ambient temperatures. The basic approach is to apply a systematic, nonperiodic distortion to the pole position distribution at the lower assembly-area temperatures, which will result in a periodic pole distribution when the structure is brought to the final operating temperature.

To construct the compensation function, the behavior of the system can be characterized as a series of expansions or contractions about nodes on the backing beam, the nodes being the center of the modules. The nodes move in accordance with the expansion and contraction of the backing beam at the expansion rate of iron while the magnetic structure modules expand or contract about these nodes at the expansion rate of aluminum.

If the end of the magnetic structure is fixed at $Z = 0$ and the ideal locations of the nodes are given by L_n for $n=0, 1, 2, \dots, 6$, and the pole locations relative to each node are given by L_p , then the compensation distortion functions D_{np} for each module are given by

$$D_{np} = C_b * \Delta T * L_n + C_m * L_p * \Delta T \quad \text{for } n = 0, 1, 2, \dots, 6 \quad (1)$$

where: p ranges from 1 to the maximum number of poles for a given module,

C_b is the coefficient of expansion of the iron backing beam,

C_m is the coefficient of expansion of the aluminum module, and

ΔT is the temperature of the structure during adjustment minus the final operating temperature.

In equation (1) above, if L_p is the location of the center pole of a given module then $L_p=0$ and the distortion value D_{np} is simply a function of the expansion of the backing beam. For all other poles the distortion function is bilinear.

When this distortion function is applied to the ideal uniform pole distribution, a new temperature-compensated ideal distribution is obtained. Measured pole position data are compared to this temperature-compensated distribution and a compensated error distribution is obtained. An example of a graph of such a distribution is shown in Figure 15. The horizontal bars in the graph delineate the magnetic structure modules and represent the average compensated longitudinal position error of the poles of a given module.

In practice this compensated error graph is used to determine the target longitudinal positions of the periodic modules on the backing beam. When the compensation function is applied at normal assembly-environment temperatures, which are some 4 degrees C cooler than the operating temperature, a contracted structure results with gaps between the modules. As the temperature is elevated the backing beam expands at its normal rate while the modules expand at a faster rate and the structure becomes uniformly periodic.

Figure 16 illustrates the intentional Z-axis distortion of the well aligned magnetic structure of Figure 15. Note the difference in vertical scale of the two graphs. The graph in Figure 16 represents the deviations from ideal periodicity of the structure at room temperature. The "stair-step" effect seen in the graph is characteristic of the low-temperature error distribution as well as the clockwise rotation of the error distributions of the individual modules. As the temperature of the structure is raised, this error distribution flattens and approaches that of Figure 15.

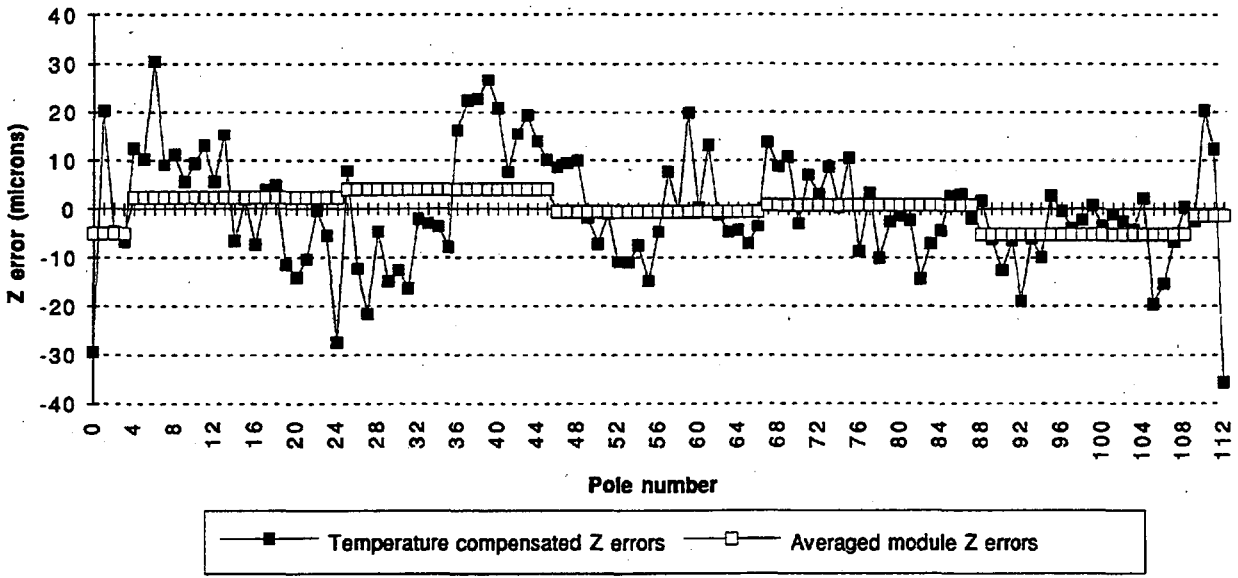


Figure 15. Laser-interferometric, temperature-compensated longitudinal (Z) error distribution with averaged error plane for each module.

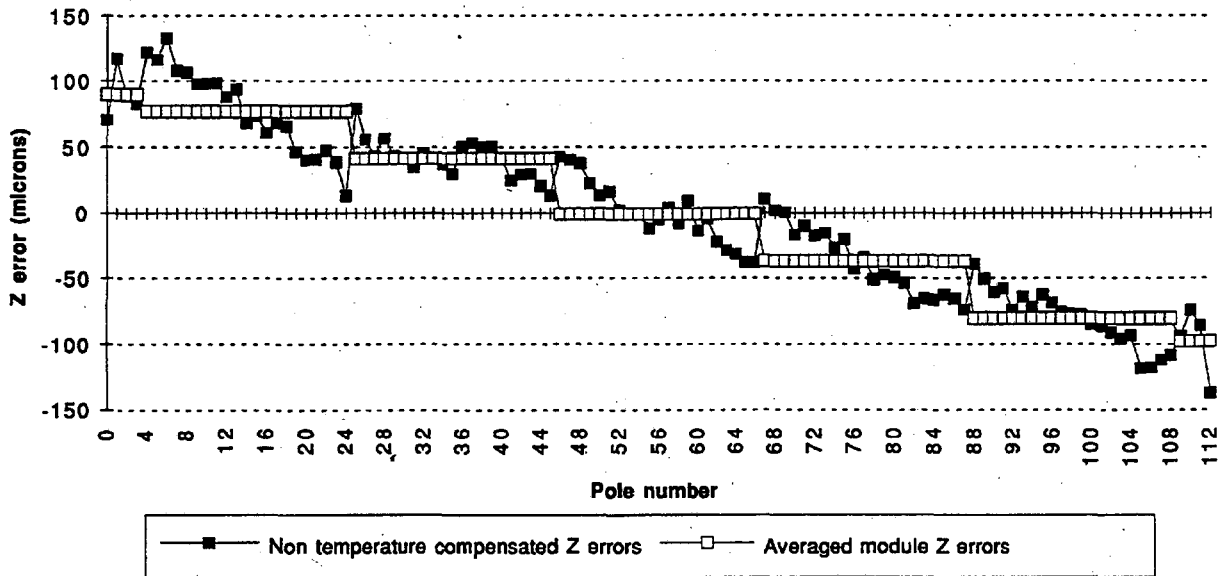


Figure 16. Laser-interferometric, non-temperature-compensated longitudinal (Z) error distribution.

This system of alignment was initially tested by applying the compensation function to measured U5.0 data taken by laser interferometer at 20 degrees C and performing the indicated distorted adjustments. The assembly room temperature was then elevated to 24 degrees C and held until the measured temperature of the magnetic structure and backing beam assembly had stabilized at the new temperature. Longitudinal pole positions were again measured with the laser system. The results indicated a reduction of *maximum* pole periodicity errors by a factor of six to the target value of 50 microns. The errors in the averaged periodic module locations were reduced to a maximum of about five microns.

5. CONCLUSIONS

Three 4.6-m devices at the Advanced Light Source have now been aligned using the techniques described in this paper. Characteristics of calculated spectra based on magnetic measurements of these devices indicate that the precision of the alignment exceeds the requirements for spectral performance.⁹ The techniques presented here have proven to be reliable and effective in producing magnetic structures which meet the precision alignment requirements of third-generation insertion devices.

6. ACKNOWLEDGEMENT

This work was supported by the Director, Office of Energy Research, Office of Basic Energy Sciences, Materials Sciences Division, of the U.S. Department of Energy under Contract No. DE-AC03-76SF00098.

6. REFERENCES

1. E. Hoyer, J. Akre, J. Chin, B. Gath, D. Humphries, B. Kincaid, S. Marks, P. Pipersky, D. Plate, G. Portmann, R. Schlueter, "First undulators for the Advanced Light Source," *IEEE PAC*, May 1993.
2. D. Humphries, "Block bonding procedure for IDA/IDB/IDC," *LBL Engineering Note M7121*, Feb 1991.
3. R. Savoy, K. Halbach, W. Hassenzahl, E. Hoyer, D. Humphries, B. Kincaid, "Calculation of magnetic error fields in hybrid insertion devices," *Nuclear Instruments and Methods in Physics Research*, A291, 1990.
4. D. Humphries, P. Pipersky, "ALS insertion device magnetic structure alignment procedure," *LBL Engineering Note M7363*, June 1993.
5. D. Humphries, E. Hoyer, B. Kincaid, S. Marks, R. Schlueter, "Magnet sorting algorithms for ALS insertion devices," *Proceedings of the Thirteenth International Conference on Magnet Technology*, to be published Sept 1993.
6. J. Chin, "IDA, IDB, IDC support and drive system assembly and alignment notes," *LBL Engineering Note M7349*, July 1992.
7. W. Gath, "Magnetic structure installation and alignment into backing beam," *LBL Engineering Note M7265*, Mar. 1992.
8. D. Humphries, "ALS insertion device magnetic structure laser interferometer measurements," *LBL Engineering Note M7364*, June 1993.
9. S. Marks, D. Humphries, B. Kincaid, R. Schlueter, C. Wang, "Analysis of insertion device magnetic measurements for the Advanced Light Source," *SPIE Proceedings Vol. 2013*, July 1993.

LAWRENCE BERKELEY LABORATORY
UNIVERSITY OF CALIFORNIA
TECHNICAL INFORMATION DEPARTMENT
BERKELEY, CALIFORNIA 94720